

# Tunnel spectroscopy in ac-driven quantum dot nanoresonators

J. Villavicencio,<sup>1,2</sup> I. Maldonado,<sup>1,3,4</sup> R. Sánchez,<sup>1</sup> E. Cota,<sup>4</sup> and G. Platero<sup>1</sup>

<sup>1</sup>*Instituto de Ciencia de Materiales de Madrid (CSIC), Cantoblanco, 28049 Madrid, Spain*

<sup>2</sup>*Facultad de Ciencias, Universidad Autónoma de Baja California, Ensenada, México*

<sup>3</sup>*Centro de Investigación Científica y de Educación Superior de Ensenada, México*

<sup>4</sup>*Centro de Nanociencias y Nanotecnología,*

*Universidad Nacional Autónoma de México, Ensenada, México*

(Dated: published online 12 May 2008)

## Abstract

Electronic transport in a triple quantum dot shuttle device in the presence of an ac field is analyzed within a fully quantum mechanical framework. A generalized density matrix formalism is used to describe the time evolution for electronic state occupations in a dissipative phonon bath. In the presence of an ac gate voltage, the electronic states are dressed by photons and the interplay between photon and vibrational sidebands produces current characteristics that obey selection rules. Varying the ac parameters allows to tune the tunneling current features. In particular, we show that coherent destruction of tunneling can be achieved in our device.

PACS numbers:

The study of nanoelectromechanical systems (NEMS) has drawn a great deal of interest, both at an applied and at a fundamental level, due to novel transport regimes arising from the strong interplay between electrical and mechanical degrees of freedom<sup>1</sup>. This is of particular interest in the field of molecular electronics where, for example, the vibrational modes of a  $C_{60}$  molecule are coupled to its charge state giving rise to new features in the current through the molecule<sup>2</sup>.

Shuttling is an example of nonlinear transport regime in NEMS, where an oscillating nano-grain acts as a shuttle carrying one electron from the left to the right contact. A paradigmatic proposal of such a device was made in the seminal work by Gorelik et al.<sup>3</sup>, and, since then, there have been different models that describe the mechanical degree of freedom using semiclassical<sup>4</sup> or quantum mechanical<sup>5,6</sup> approaches. In the presence of an ac electric field, it is known that the interplay between the ac and the natural frequency of the device gives rise to rich dynamics with strong nonlinear characteristics. These can be modified by tuning the ratio of the two frequencies or the intensity of the applied field. Up to now, this problem has been addressed for the case of an oscillating quantum dot (QD) using a semiclassical approach to describe the oscillations<sup>4</sup>.

In this letter we introduce a full quantum mechanical description to study the dynamics of a triple dot quantum shuttle (TDQS) with an ac gate voltage applied between the different QDs and including quantum optical damping as a dissipation bath<sup>5</sup>. Using the master equation approach for the reduced density matrix (RDM), we show how tunneling current resonances occur through different combinations of photonic and phononic sidebands and derive sum rules to explain these resonances. These features strongly depend on the ratio between the frequency and intensity of the ac field. Thus, by tuning the ac frequency we can obtain information on the vibrational frequency of the resonator. Finally, we find that the ac parameters can be manipulated so that coherent destruction of tunneling<sup>7,8</sup> (CDT) can be observed.

We consider a TDQS, which consists of an array of three QDs where the central movable dot is flanked by two static dots at fixed positions  $\pm x_0$ . The oscillation of the central dot will affect the tunneling rates, which are now position dependent. The charge transport is within the Coulomb blockade regime, so the charging energy is assumed to be sufficiently large that only one transport electron can occupy the chain of three dots at any given time. Our model introduces a time-dependent ac potential  $V(t) = V_{ac} \cos(\omega_{ac}t)$ , applied between

the left and right QDs, where  $V_{ac}$  and  $\omega_{ac}$  are the amplitude and frequency of the applied field, respectively (see Fig. 1). The system is modeled by means of a Hubbard like Hamiltonian,  $\hat{H} = \hat{H}_{TQS} + \hat{H}_{leads}$ , where the unperturbed hamiltonian is  $\hat{H}_{TQS} = \hat{H}_0 + \hat{H}_{osc} + \hat{H}_{tun} + \hat{H}_{ac}$ , where  $\hat{H}_0 = \sum_s \varepsilon_s c_s^\dagger c_s$  represents the Hamiltonian of the left-hand ( $l$ ), central ( $c$ ), and right-hand ( $r$ ) dots, for spinless electrons with respective localized states  $\varepsilon_s$  ( $s = l, c, r$ ). The energy of the central QD is  $\varepsilon_c(\hat{x}) = [\varepsilon_l - (\varepsilon_b/2x_0)(\hat{x} + x_0)]$ , where it is assumed that it undergoes a Stark shift proportional to its position due to the voltage bias across the device  $\varepsilon_b = (\varepsilon_l - \varepsilon_r)$ ;  $\hat{H}_{osc} = \hbar\omega d^\dagger d$  is the energy associated to the oscillation of the central QD, with frequency  $\omega$ .  $\hat{H}_{tun} = \sum_{s'=l,r} T_{s'}(\hat{x}) [c_s^\dagger c_{s'} + h.c.]$ , represents the tunneling between all three dots, with position dependent tunneling rates  $T_l = -V \exp^{-\alpha(x_0 + \hat{x})}$ , and  $T_r = -V \exp^{-\alpha(x_0 - \hat{x})}$ , where  $V$  is the tunneling amplitude and  $\alpha$  is the inverse of the tunneling length. The position operator  $\hat{x}$  measures the displacement of the vibrational mode and is given by  $\hat{x} = \Delta x_{zp} (\hat{d}^\dagger + \hat{d})$ , where  $\Delta x_{zp} = (\hbar/2m\omega)^{1/2}$  is the zero-point uncertainty position of the oscillator.  $\hat{H}_{ac} = (V_{ac}/2) \cos(\omega_{ac}t) (c_l^\dagger c_l - c_r^\dagger c_r)$ , provides the effect of the ac potential, which is introduced as an oscillation of opposite phase on the energy levels of the right and left dots flanking the central dot and  $\hat{H}_{leads} = \sum_\alpha \sum_{k_\alpha, \sigma} \epsilon_{k_\alpha} c_{k_\alpha \sigma}^\dagger c_{k_\alpha \sigma}$ . The equation of motion of the system using the standard RDM approach<sup>9</sup>, generalized to include the environment of the oscillator, is given by:  $\dot{\rho}_{qs}^{ij} = (\dot{\rho}_{qs}^{ij})_{RDM} + (\dot{\rho}_{qs}^{ij})_{diss}$ , where  $\rho_{qs}^{ij}$  represents the matrix element with the dot states  $q$  and  $s$  ( $q, s = 0, l, c, r$ ), with the oscillator states  $i$ , and  $j$  ( $i, j = 0, 1, 2, \dots$ ). The term  $(\dot{\rho}_{qs}^{ij})_{RDM}$  incorporates transitions between the leads and the outer dots:

$$\begin{aligned}
(\dot{\rho}_{qs}^{ij})_{RDM} &= -\frac{i}{\hbar} [\hat{H}, \rho]_{qs}^{ij} \\
&+ \begin{cases} \sum_{d \neq q} (\Gamma_{d \rightarrow q} \rho_{dd}^{ij} - \Gamma_{q \rightarrow d} \rho_{qq}^{ij}); & q = s \\ -\frac{1}{2} \left( \sum_{d \neq q} \Gamma_{q \rightarrow d} + \sum_{d \neq s} \Gamma_{s \rightarrow d} \right) \rho_{qs}^{ij}; & q \neq s. \end{cases} \quad (1)
\end{aligned}$$

Here we have also considered the transitions  $\Gamma_{r \rightarrow 0} = \Gamma_{0 \rightarrow l} = \Gamma$ . The term  $[\dot{\rho}_{qs}^{ij}]_{diss}$  accounts for the dissipative effects of the oscillator's environment. We assume a damping model composed of a bath of oscillators at a fixed temperature  $T$ , to which the vibrational mode is weakly coupled<sup>10</sup>. In the limit of small values of  $T$ , the matrix elements are given by  $[\dot{\rho}_{qs}^{ij}]_{diss} = -\gamma[(i+j)/2]\rho_{qs}^{ij} + \gamma[(i+1)(j+1)]^{1/2}\rho_{qs}^{i+1, j+1}$ , where  $\gamma$  is the classical damping rate of the oscillator. Finally, the matrix elements of the tunneling amplitudes  $T_{l,r}^{ij}$  in the oscillator basis can be computed.

In what follows, we shall explore the main features of the current  $I_{ac}$  for a TDQS driven by an ac gate voltage. We have considered weak coupling between the three QDs, a regime characterized by large values of  $\alpha$ . The calculations are performed by numerical integration of the RDM and averaging over the resulting electronic current measured at the right QD, i.e.,  $I_{ac} = e \Gamma \sum_i [\rho_{rr}^{ii}]_{av}$ . We begin our analysis by exploring  $I_{ac}$  as a function of the bias  $\varepsilon_b$  for different values of the ac parameters. All of the calculations are worked out in units where  $\hbar = 2m = \omega = e = 1$  and  $N = 6$  oscillator states were included. For the particular values of the voltage bias across the device  $\varepsilon_b$  considered in our calculations, we have numerically verified that including more oscillator states does not significantly change the current characteristics for typical experimental parameters. In Fig. 2(a) we plot the time-averaged current  $I_{ac}$  (solid line) for a particular value of the ratio  $\xi = (V_{ac}/2\omega_{ac}) = 3.0$ , where  $\omega = p\omega_{ac}$  ( $p$  integer). We can appreciate a much richer structure for  $I_{ac}$  than the undriven case (dashed line). We find a series of peaks or maxima appearing at specific values of  $\varepsilon_b$ , which are integer multiples of  $\omega_{ac}$ , and obeying the following sum rules:

$$\varepsilon_b + \nu\hbar\omega_{ac} = n\hbar\omega, \quad (2)$$

$$(\varepsilon_b/2) + \nu\hbar\omega_{ac} = n\hbar\omega. \quad (3)$$

Here,  $n$  corresponds to the vibrational level at which the transmitted electron ends up in the right dot, and  $\nu$  to the number of emitted or absorbed photons needed to reach that vibrational level. The peaks that satisfy the sum rule of Eq. (2) are positioned at a value of  $\varepsilon_b$  equal to an *odd* multiple of  $\omega_{ac}$ , and are identified by  $[\nu, n]$ . These correspond to an alignment between photon-assisted tunneling (PAT) sidebands of the vibrational resonator states of the right and left dots. As in the undriven case, these peaks are suppressed in the very weak coupling regime. The peaks satisfying Eq. (3), positioned at an *even* multiple of  $\omega_{ac}$ , are identified with  $(\nu, n)$ , and correspond to alignment of sidebands of all three dots. In order to further corroborate the label assignments, we calculate the occupation probabilities for the right QD  $\rho_{rr}^{ii}$ , which determine  $I_{ac}$ . In Fig. 2(b), we present the results corresponding to the peak at  $\varepsilon_b \simeq 0.4$  [with labels  $(-1, 0), (+4, 1)$ ], where we can clearly see that the most important contribution arises from  $\rho_{rr}^{00}$ . Similarly, for all the resonances we have verified that the most important contribution comes from the satellite with the least number of photons, which is consistent with a low field intensity.

In what follows we shall introduce a useful transformation in order to demonstrate that the different peaks associated to the PAT current are in fact associated with the emission or absorption of  $\nu$  photons. Performing a unitary transformation<sup>11</sup>  $\hat{U} = \exp \left[ -i(V_{ac}/2\omega_{ac}) \sin(\omega_{ac}t)(c_l^\dagger c_l - c_r^\dagger c_r) \right]$  on the Hamiltonian  $\hat{H}$ , leads to a transformed tunneling Hamiltonian  $\hat{H}'_{tun}$  with time dependent tunneling amplitudes  $\tilde{T}_l = T_l \sum_{\nu=-\infty}^{\nu=+\infty} (-1)^\nu J_\nu(\xi) e^{i\omega_{ac}\nu t}$ , and  $\tilde{T}_r = T_r \sum_{\nu=-\infty}^{\nu=+\infty} (-1)^\nu J_\nu(\xi) e^{-i\omega_{ac}\nu t}$ . Thus, the tunneling amplitudes become renormalized by a sum of Bessel functions of order  $\nu$ , where  $\nu$  is the number of absorbed or emitted photons. By computing the current using this approach we obtain an excellent agreement with our previous calculation. The peaks in  $I_{ac}$  can be explained by an interplay of the vibrational and photoassisted sidebands as follows: the TDQS can be seen as a system of three fixed QDs, whose energy levels are separated by  $(\varepsilon_b/2)$ , and the effect of the oscillator is to split these energies into vibrational satellite sub-bands separated by the vibrational energy  $\hbar\omega$ . When the ac voltage is applied across the device, an additional level splitting of their energies occurs by an amount of  $\hbar\omega_{ac}$ , giving rise to new conduction channels (resonances) which are accurately described by the sum rules.

We can now exploit the analytical properties of the Bessel functions in order to control the current characteristics by an adequate manipulation of the ac parameters. In Fig. 3 we use  $\xi = 2.405$ , for  $\omega_{ac} = 0.2$  and a lower  $V_{ac} = 0.96192$ , corresponding to the first zero of  $J_0(\xi)$ . In this case, direct tunneling processes involving  $\nu = 0$  at  $\varepsilon_b \simeq 0.0, 2.0$ , are suppressed due to CDT<sup>7,8</sup>. Here, the energy levels of the vibrational subbands of the three dots are aligned, but  $\tilde{T}_l \approx 0$  and  $\tilde{T}_r \approx 0$ . Note that these values of  $\varepsilon_b$  also correspond to resonances in the undriven case. Interestingly, the current peaks at  $\varepsilon_b \simeq 0.6, 1.0$ , and  $1.4$  [with labels  $[\nu, n]$ ], observed in Fig. 2, are also significantly diminished. This decrease in the current is due to two factors: the small overlap of the wave functions in both left and right QDs and the decrease in the intensity of the ac field, which yield a small probability for processes involving several photons. We see that the main peaks are governed by the emission and absorption of several photons ( $\nu = \pm 4, \dots, \pm 1$ ) and correspond to alignment of the levels of all three dots.

In conclusion, we have analyzed the characteristics of the electronic current in an ac driven TDQS device using a full quantum mechanical approach. Our results show that by tuning the ac field parameters we can control the current contribution from differently vibrational modes. This constitutes a new mechanism to obtain information on vibrational

modes through current measurements as for example in the context of molecular shuttle devices.

We acknowledge A. Donarini for helpful discussions. This work has been supported by the MCYT (Spain) under grant MAT2005-06444, and by the EU Programme HPRN-CT-2000-00144. J.V. acknowledges support from MEC-Spain: SB2005-0047. I.M. and E.C. acknowledge support from CONACyT, México, 43673-F.

- 
- <sup>1</sup> L. Y. Gorelik, A. Isacsson, Y. M. Galperin, R. I. Shekhter, and M. Jonson, *Nature (London)* **411**, 454 (2001); V. Sazonova Y. Yaish, H. Üstünel, D. Roundy, T. A. Arias, and P. L. McEuen, *ibid.* **431**, 284 (2004); D. V. Scheible and R. H. Blick, *Appl. Phys. Lett.* **84**, 4632 (2004).
- <sup>2</sup> H. Park, J. Park, A. K. L. Lim, E. H. Anderson, A. P. Alivisatos, and P. L. McEuen, *Nature (London)* **407**, 57 (2000).
- <sup>3</sup> L. Y. Gorelik, A. Isacsson, M. V. Voinova, B. Kasemo, R. I. Shekhter, and M. Jonson, *Phys. Rev. Lett.* **80**, 4526 (1998).
- <sup>4</sup> F. Pistolesi, *Phys. Rev. B* **69**, 245409 (2004); F. Pistolesi and R. Fazio, *Phys. Rev. Lett.* **94**, 036806 (2005).
- <sup>5</sup> A. D. Armour and A. MacKinnon, *Phys. Rev. B* **66**, 035333 (2002).
- <sup>6</sup> C. Flindt, T. Novotný, and A.-P. Jauho, *Phys. Rev. B* **70**, 205334 (2004); T. Novotný, A. Donarini, and A.-P. Jauho, *Phys. Rev. Lett.* **90**, 256801 (2003).
- <sup>7</sup> F. Grossmann, T. Dittrich, P. Jung, and P. Hänggi, *Phys. Rev. Lett.* **67**, 516 (1991).
- <sup>8</sup> G. Platero and R. Aguado, *Phys. Rep.* **395**, 1 (2004); C. E. Creffield and G. Platero, *Phys. Rev. B* **65**, 113304 (2002).
- <sup>9</sup> K. Blum, *Density Matrix Theory and Applications* (Plenum, N. Y. 1996).
- <sup>10</sup> M. O. Scully and M. S. Zubairy, *Quantum Optics* (Cambridge University Press, Cambridge, U.K., 1997).
- <sup>11</sup> R. Sánchez and G. Platero, *Mathematics in Industry*, edited by L. L. Bonilla, M. A. Moscoso, G. Platero, and J. M. Vega (Springer, Berlin, 2007), Vol. 12 p. 444.

FIG. 1: Driven TDQS where oscillating tunneling barriers between the central quantum dot and its neighbors are considered. The system is driven by an ac potential  $V(t) = V_{ac} \cos(\omega_{ac}t)$  and the left and right tunneling barriers are rigidly coupled to the leads.

FIG. 2: (Color online) (a)  $I_{ac}$  (in units of  $\Gamma$ ) vs  $\varepsilon_b$  (blue solid line) for the ac parameters  $\omega_{ac} = 0.2$ , and  $V_{ac} = 1.2$ , and typical values of the parameters  $\{V, \gamma, x_0, \Gamma, \alpha\} = \{0.5, 0.01, 5.0, 0.05, 0.4\}$ . The red dashed line corresponds to  $I_{ac}$  in the undriven case. The ac current peaks are labeled with  $[\nu, n]$ , and  $(\nu, n)$ , associated to the sum rules given by Eqs. (2), and (3), respectively. In (b) we show the occupation probabilities of the right dot  $\rho_{rr}^{ii}$ , for  $i = 0$  (green line),  $i = 1$  (red dashed line), and  $i = 2$  (blue dotted line), as a function of time, corresponding to the current peak at  $\varepsilon_b \simeq 0.4$ .

FIG. 3: (Color online)  $I_{ac}$  (in units of  $\Gamma$ ) as a function of  $\varepsilon_b$  (blue solid line), for  $\omega_{ac} = 0.2$ ,  $V_{ac} = 0.96192$  ( $\xi = 2.405$ ), corresponding to the first zero of  $J_0(\xi)$ , showing CDT. Parameters for the undriven case (dotted line) are the same as in the previous figure.



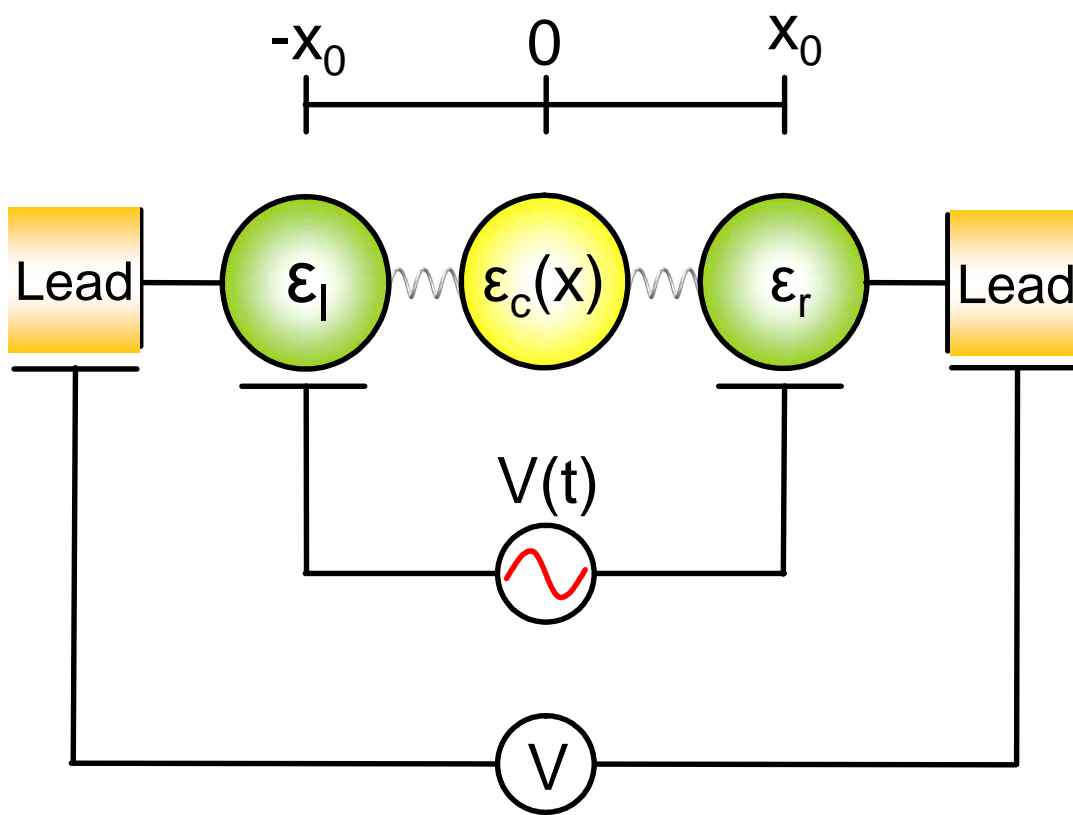


Figure 1

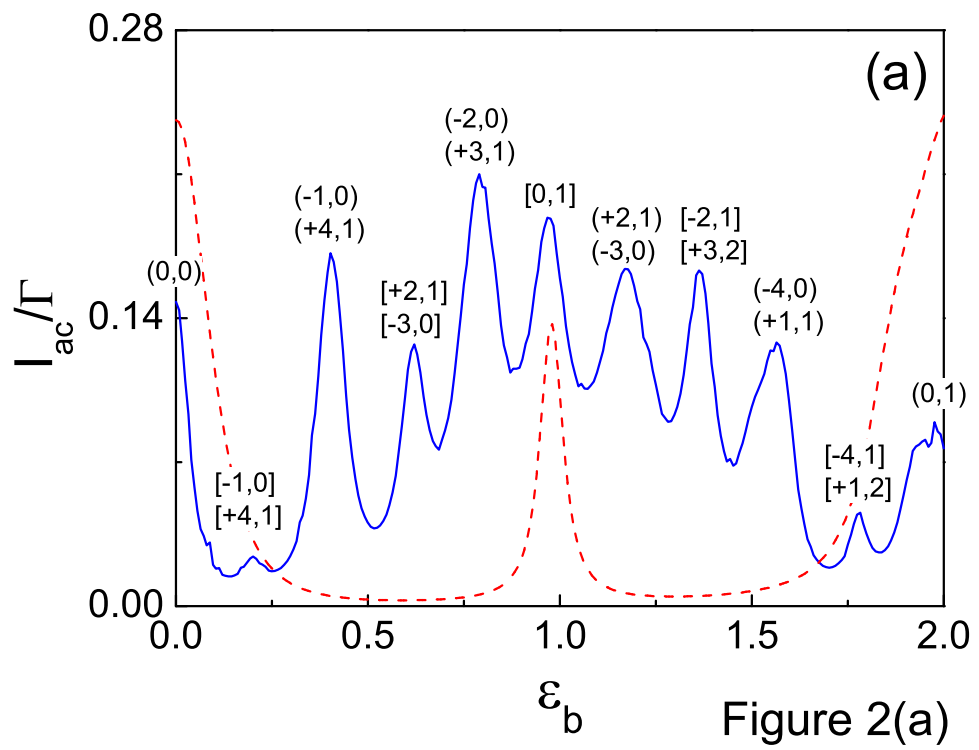


Figure 2(a)

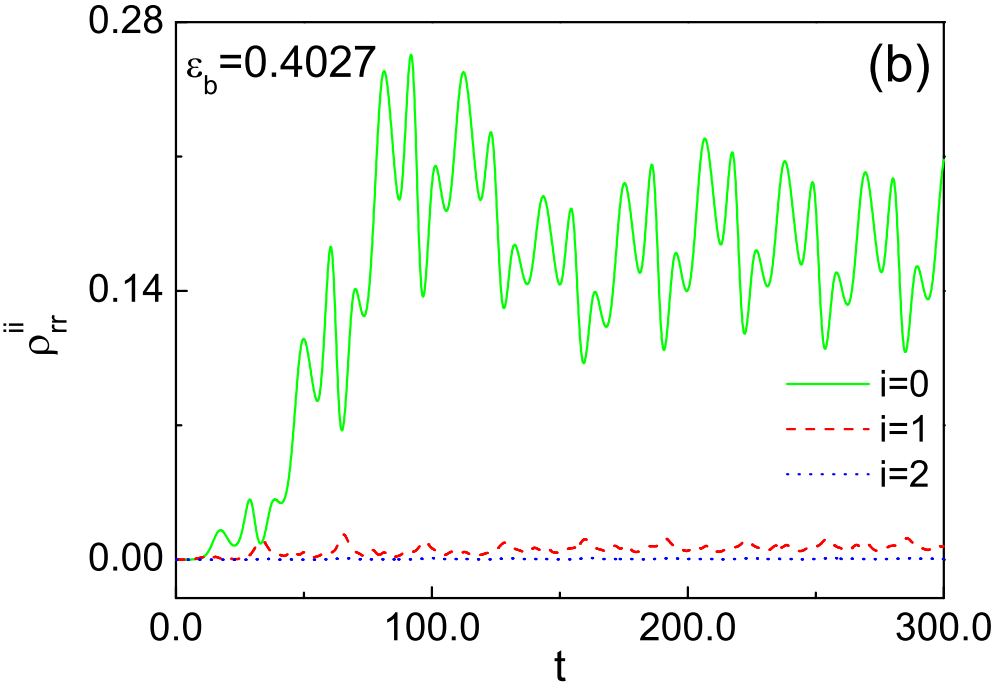


Figure 2(b)

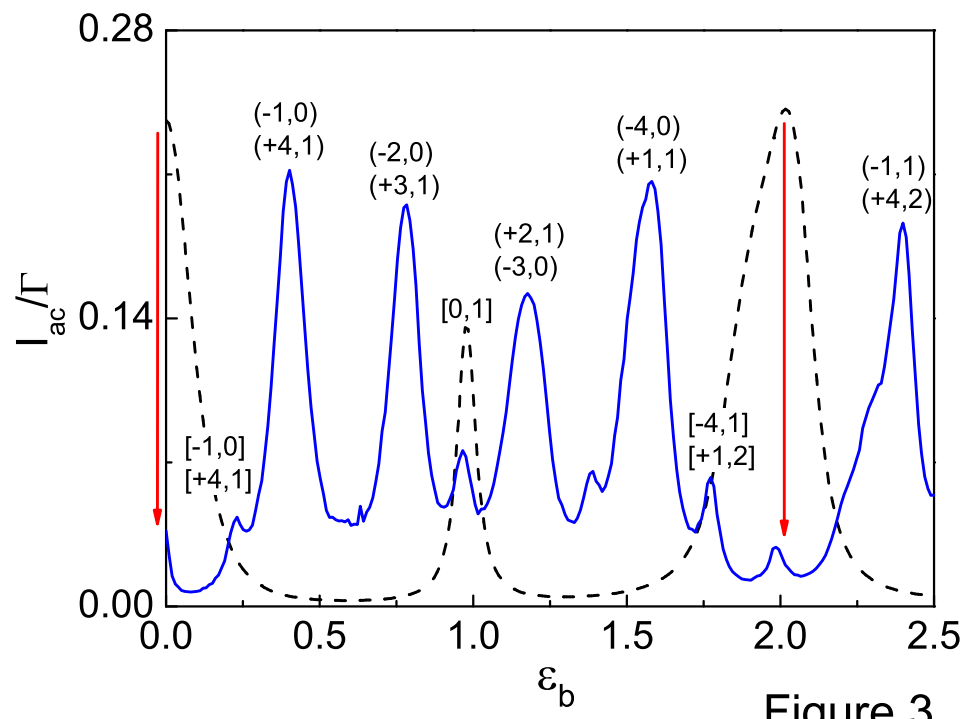


Figure 3